AGU100 ADVANCING EARTH AND SPACE SCIENCE

Geophysical Research Letters

RESEARCH LETTER
10.1029/2018GL077000

Key Points:
- Direct observations of meltwater export from a major Greenland glacial fjord are reported
- Properties of the exported meltwater mixture are dominated by entrainment and upwelling
- Noble gases reveal the vertical structure of Greenland meltwater forcing of the coastal ocean

Supporting Information:
- Supporting Information S1

Correspondence to:
N. L. Beaird,
nbeaird@whoi.edu

Citation:
Beaird, N. L., Straneo, F., & Jenkins, W. (2018). Export of strongly diluted Greenland meltwater from a major glacial fjord. *Geophysical Research Letters*, *45*, 4163–4170. https://doi.org/10.1029/2018GL077000

Received 2 JAN 2018
Accepted 7 APR 2018
Accepted article online 19 APR 2018
Published online 5 MAY 2018

Export of Strongly Diluted Greenland Meltwater From a Major Glacial Fjord

Nicholas L. Beaird[1], **Fiammetta Straneo**[2], **and William Jenkins**[3]

[1]Physical Oceanography Department, Woods Hole Oceanographic Institution, Woods Hole, MA, USA, [2]Scripps Institution of Oceanography, La Jolla, CAUSA, [3]Department of Marine Chemistry and Geochemistry, Woods Hole Oceanographic Institution, Woods Hole, MA, USA

Abstract The Greenland Ice Sheet has been, and will continue, losing mass at an accelerating rate. The influence of this anomalous meltwater discharge on the regional and large-scale ocean could be considerable but remains poorly understood. This uncertainty is in part a consequence of challenges in observing water mass transformation and meltwater spreading in coastal Greenland. Here we use tracer observations that enable unprecedented quantification of the export, mixing, and vertical distribution of meltwaters leaving one of Greenland's major glacial fjords. We find that the primarily subsurface meltwater input results in the upwelling of the deep fjord waters and an export of a meltwater/deepwater mixture that is 30 times larger than the initial meltwater release. Using these tracer data, the vertical structure of Greenland's summer meltwater export is defined for the first time showing that half the meltwater export occurs below 65 m.

Plain Language Summary The Greenland Ice Sheet has been melting at an accelerating pace. As it melts, more and more freshwater drains into the Northern North Atlantic. This may have significant impacts on ocean circulation. In order to start to understand these impacts, we need better observations of the spreading of ice sheet meltwater around coastal Greenland. In this work we use noble gases as a natural "dye" that traces out the pathways of ice melt in coastal waters. These "dyes" give us a powerful tool to measure the size and location of ice melt export. This paper quantifies the flux of two types of meltwater in a major East Greenland fjord and shows that the meltwater is highly diluted by mixing with warm, salty waters from the deepest part of the fjord. Showing which ocean waters dilute the glacial melt is one step toward better representing these processes in numerical models.

1. Introduction

The subpolar North Atlantic forms a critical link in the climate system where wintertime deep convection indirectly connects the upper and lower branches of the Atlantic Meridional Overturning Circulation (Lozier, 2012). This convective link is sensitive to surface stratification and thus to variability in freshwater sources (Lazier, 1980; Manabe, 1995). Greenland, which sits adjacent to the convective areas of the subpolar gyre, not only is an increasing source of freshwater (Bamber et al., 2012; Fettweis et al., 2012; Shepherd et al., 2012) but also steers the export of a large volume of freshwater and sea ice from the Arctic via boundary currents that circulate around the island (Sutherland et al., 2009). Thus, processes influencing freshwater transport and transformation along the coast of Greenland may impact climate through interactions with subpolar gyre convection and the Atlantic Meridional Overturning Circulation. However, observations of the magnitude and structure of meltwater spreading around coastal Greenland are extremely limited. Here we use novel tracer methods to characterize glacier-driven water mass transformation and make robust estimates of meltwater export in a major Greenland fjord.

Meltwater from Greenland enters the ocean at marine-terminating glaciers and rivers sourced from land-terminating glaciers (Chu, 2014). Recent Greenland mass loss is nearly equally partitioned between increased ice discharge and enhanced surface melt (van den Broeke et al., 2009), and roughly three quarters of the total mass loss is routed through marine-terminating glaciers—making them an important source of the anomalous freshwater flux into the ocean. Marine-terminating glaciers produce submarine meltwater (submarine ice melt by ocean heat) and subglacial discharge (surface melt release at depth at the glacier's

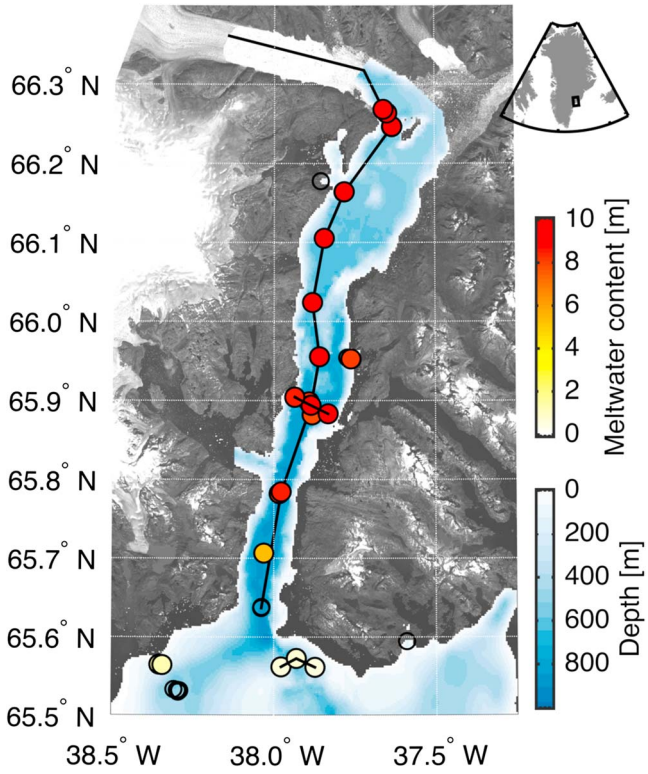

Figure 1. August 2015 survey and meltwater content in Sermilik Fjord. Landsat image of Sermilik with bathymetry (blue) and 2015 station locations (circles). Colored circles mark stations where noble gas samples were taken. Color corresponds to the vertically integrated total meltwater content (subglacial discharge + submarine meltwater) reported as a thickness in meters. Black lines indicate the sections shown in Figures 2 and 3.

grounding line; Straneo & Cenedese, 2015). In addition, icebergs calved from glaciers can lose much of their mass from ocean-driven melting in the vicinity of glacier termini (Enderlin et al., 2016)—contributing substantially to the total meltwater export from the fjord (Moon et al., 2018).

A key feature of marine-terminating glaciers is that in contrast to land-terminating glaciers, meltwaters are injected not at the surface but distributed throughout depth in stratified fjord waters. This subsurface buoyancy input generates convective turbulent plumes at the ice-ocean interface (Carroll et al., 2015; Straneo & Cenedese, 2015). Entrainment and mixing in the plumes transforms the initial freshwater flux from the ice sheet into a much larger volume flux of "glacially modified water"—the mixture of glacial freshwater and entrained ocean water whose properties ultimately influence the coastal and regional ocean. In order to assess the impact of increased Greenland melt on the ocean, it is critical to understand and properly represent the transformation processes that create glacially modified water.

The mixing and entrainment that create glacially modified waters occur in thin boundary layers at the ice/ocean interface and, thus far, have been prohibitively difficult to observe directly (Jackson et al., 2017; Mankoff et al., 2016). Yet improved understanding of their net effect can be gained from observations of the resulting distribution, export, and dilution of submarine meltwater and subglacial discharge away from the boundary. Standard hydrographic measurements of temperature and salinity alone, however, are insufficient to quantify submarine meltwater and subglacial discharge distributions (Beaird et al., 2015). In contrast, dissolved noble gas observations provide additional constraints that enable robust estimates of the concentration of subglacial discharge and submarine meltwater (Hohmann et al., 2002; Loose & Jenkins, 2014; Schlosser, 1986). In conjunction with velocity, these can be used to infer the spreading and export of subglacial discharge, submarine meltwater, and glacially modified water in general. These tracer observations provide a powerful way to make comprehensive observations of meltwater export, and overcome the deficiencies associated with previous methods that rely on poorly constrained heat and salt budgets and/or water mass analysis. We report results from Sermilik Fjord (Figure 1), at the marine terminus of Helheim Glacier.

Helheim is one of Greenland's largest outlet glaciers and has, along with four other large glaciers, contributed over 50% of the ice sheet discharge anomaly since 2000 (Enderlin et al., 2014). The total ice discharge into Sermilik Fjord is estimated to be 1,100 $m^3\ s^{-1}$ (Mernild et al., 2010), and the peak summer subglacial discharge estimated from a regional climate model (Moon et al., 2018; Noël et al., 2016) is 1,800 $m^3\ s^{-1}$, and an ocean heat and salt budget (Jackson & Straneo, 2016) gives a late-summer average of 1,200 $m^3\ s^{-1}$. The fjord is long (90 km), narrow (5–10 km), and deep (530–800 m) with no shallow sill. Sermilik opens onto the shelf where the East Greenland Coastal Current flows south carrying freshwater from the Arctic (Harden et al., 2014; Sutherland & Pickart, 2008). In nonsummer months, the fjord circulation is dominated by external forcing (Jackson et al., 2014), but in the summer a glacial buoyancy-forced estuarine circulation develops (Jackson & Straneo, 2016).

2. Meltwater Distribution in Sermilik Fjord

Glacial meltwater is injected into stratified waters composed of three ambient oceanic water types (Straneo et al., 2012; Sutherland & Straneo, 2012): deep warm/salty Atlantic Water underneath a cold/fresh Polar Water layer, capped by a thin near-surface seasonal thermocline of warm/fresh Surface Water. Atlantic Water fills the deep fjord, and previous studies have assumed Polar Water dominates the upper layer (Straneo et al., 2010, 2011; Sutherland & Straneo, 2012), though the results we present here demonstrate that in summer, this is not the case.

Hydrography and dissolved noble gas concentrations were collected throughout the fjord and adjacent shelf in 2015 (Figures 1 and 2). Inert noble gases are effective tracers of ocean-glacier interaction because of their range of solubilities, varying solubility temperature-dependance, and the presence of trapped air in glacial ice (Loose & Jenkins, 2014). Light noble gases (helium and neon) are particularly strong tracers of submarine meltwater because relative to the equilibrated ocean, they are present in very large quantities in glacial ice—pure glacial meltwater has 1,400% of the helium and 940% of the neon of background ocean waters (Schlosser, 1986). Indeed, helium (and neon, Figure S3 in the supporting information) is highly supersaturated in the fjord relative to the shelf (Figure 2), demonstrating the large submarine meltwater content of the fjord waters. This submarine meltwater can originate at the glacier terminus or along the submerged surface of icebergs—the two are indistinguishable by our method.

The noble gases in combination with temperature and salinity can be used in a linear mixing model with defined end-members (Optimum Multiparameter Analysis; Tomczak & Large, 1989) to quantify the distributions of submarine meltwater, subglacial discharge, and entrained oceanic water masses (see supporting information and Loose & Jenkins, 2014; Beaird et al., 2015, 2017). Because the number of constraints (temperature, salinity, ^{3}helium, ^{4}helium, neon, argon, krypton, xenon, and mass conservation) exceeded the number of unknowns (Atlantic, polar, and surface waters plus submarine meltwater and subglacial discharge) the linear mixing model is overconstrained (see supporting information for full details). The noble gas constraints thus permit quantitative evaluation of glacial meltwater content—resolving the primary deficiency of previous analyses based solely on temperature and salinity.

Our analysis reveals submarine meltwater and subglacial discharge spread throughout the fjord in a single 250-m-thick layer extending well below the sea surface (Figure 3). The observed single layer is in contrast to some other fjord studies reporting a multilayer spreading of meltwater (Beaird et al., 2015; Sciascia et al., 2013; Straneo et al., 2011) and emphasizes the extent to which meltwater export is not constrained to the surface. Concentrations of both meltwater types are highest at the surface where subglacial discharge concentrations exceed submarine meltwater concentrations. The submarine meltwater extends deeper than the subglacial discharge layer. The submarine meltwater and subglacial discharge layer coincides with high concentrations of Atlantic Water that has been displaced upward relative to its position on the shelf (Figures 3e and 3f). The upward Atlantic Water displacement reflects upwelling induced by entrainment in meltwater-driven convective plumes and shows that the Atlantic Water, rather than Polar Water, sets the properties of the upper layer of the fjord in summer.

A cross-fjord tilt in the isopycnals and meltwater distributions leads to thicker layers of meltwater on the west side of the fjord—consistent with a rotationally influenced export of meltwater (Figures 3i and 3j). Little submarine meltwater or subglacial discharge is found on the shelf east of the fjord (Figures 3a and 3c) upstream with respect to the East Greenland Coastal Current (Harden et al., 2014). The vertically integrated combined submarine meltwater and subglacial discharge content is about 10 m within the fjord (Figure 1).

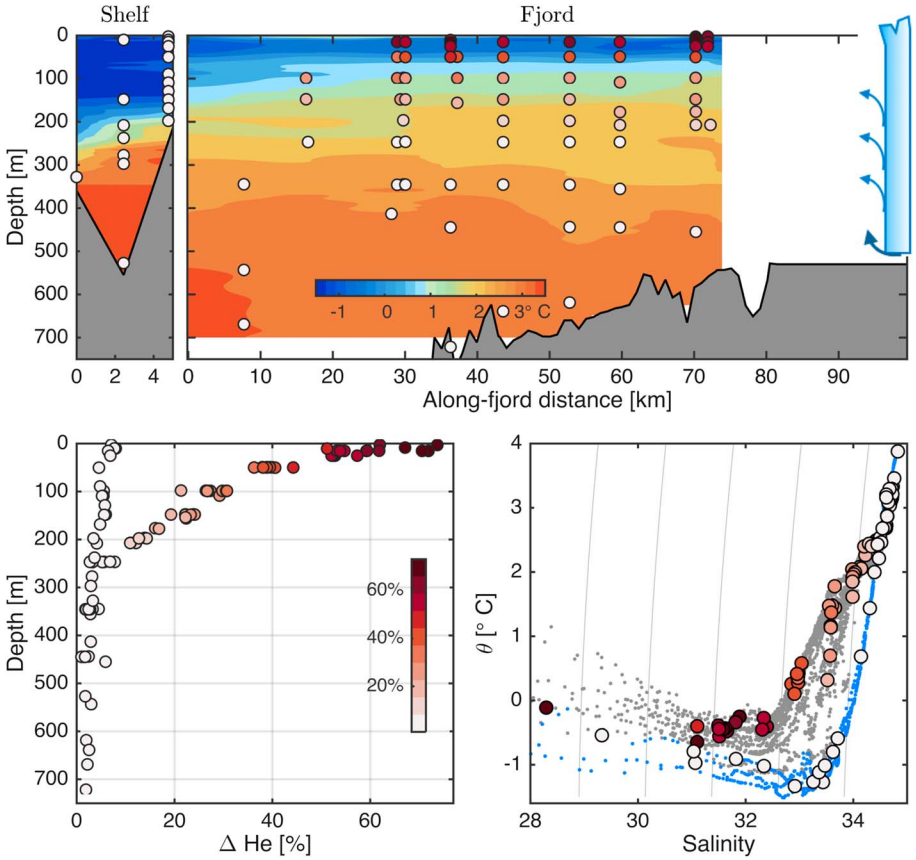

Figure 2. Hydrography and meltwater tracers. Top: Shelf and along-fjord section of temperature (contours) and Helium saturation anomaly (ΔHe, circles). Bottom: (left) depth profiles of ΔHe and (right) ΔHe plotted in potential temperature-salinity space (shelf temperature-salinity curves in blue and fjord curves in gray).

3. Meltwater Export

Observations of the export and composition of meltwater mixtures in proglacial fjords are crucial to understanding the impact of ice loss on the ocean. However, making reliable estimates of the export of Greenland meltwater with synoptic sections and standard hydrography is difficult. Without quantitative estimates of subglacial discharge and submarine meltwater concentration, meltwater transports are calculated from heat and salt budgets that often must neglect important terms such as heat storage and also result in bulk export estimates rather than a description of the vertical structure of meltwater export (Jackson & Straneo, 2016). The noble gas analysis used here permits a robust direct estimate of the vertically resolved synoptic meltwater export that does not rely on assumptions balancing poorly constrained heat and salt flux measurements with meltwater injection.

Along-fjord geostrophic velocities (supporting information section S6) at midfjord reveal a two-layer exchange with inflow toward the glacier below 250 m and outflow toward the shelf above (Figure 3i). Upper and lower layer speeds are $\approx$5 cm s^{-1}. The fjord is known to exhibit rapidly fluctuating velocities (Jackson et al., 2014); however, variability is reduced in summer (Jackson & Straneo, 2016). The structure, shear, and magnitude of the synoptically measured exchange flow agree with summer average velocities recorded by moored Acoustic Doppler Current Profilers (ADCP) at midfjord (SI).

The upper layer flow exports glacially modified water, while the lower layer imports unmodified ambient waters (Figures 3i–3k). Multiplying the meltwater distributions obtained from the noble gas analysis (Figures 3j and 3k) with the geostrophic velocity section (Figure 3i), we find an export of $1,300 \pm 100$ m^3 s^{-1} and 800 ± 500 m^3 s^{-1} of submarine meltwater and subglacial discharge respectively (Figure 4 and supporting information section S6). These are among the first robust direct measurements of synoptic meltwater flux from a glacial fjord in Greenland. They fall within the range of bulk estimates from budgets constrained by moored

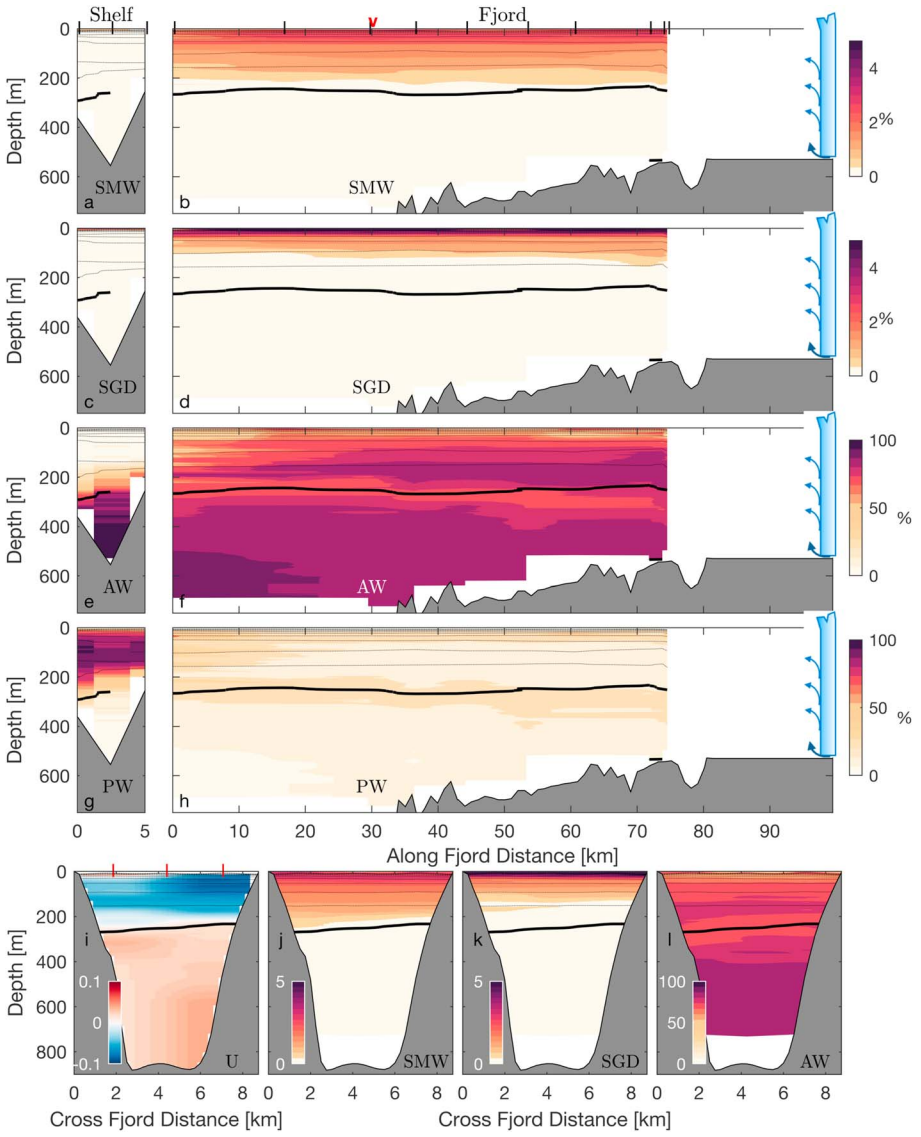

Figure 3. Greenland meltwater distribution in the fjord. (a–h) Shelf and along-fjord distributions of submarine meltwater (SMW), subglacial discharge (SGD), Atlantic Water (AW), and Polar Water (PW) content as a percentage. (i–l) Cross-fjord section at 65.9°N (at red "v" in b) of along-fjord geostrophic velocity (m s^{-1}, i) and submarine meltwater, subglacial discharge, and Atlantic Water percentages. In each panel salinity is contoured in black in 0.5 increments, and the bold contour is at 34.5. Tick marks on the top of panels a, b, and i indicate station locations.

observations in Sermilik ($1,200 \pm 700$ m^3 s^{-1} of subglacial discharge and $1,500 \pm 500$ m^3 s^{-1} of submarine melt, Jackson and Straneo, 2016) and with modeled estimates of terminus and iceberg melt (1,025 m^3 s^{-1} of submarine melt, Moon et al., 2018). Our submarine meltwater transport estimate is a combination of iceberg and terminus melt. The total export is significantly larger than estimates of terminus melt (150 m^3 s^{-1}; (Moon et al., 2018)). Thus, these results provide directly measured meltwater fluxes that support the idea that iceberg melting is a significant contributor to fjord freshwater budgets (Enderlin et al., 2016; Jackson & Straneo, 2016; Moon et al., 2018).

4. Entrainment, Overturning, and Production of Glacially Modified Waters

Low concentrations of subglacial discharge (maximum 6%) and submarine meltwater (maximum 3.25%) found in the fjord (supporting information Figure S7) demonstrate that ice sheet meltwaters are highly diluted, emphasizing the dominant role of entrainment in setting the properties of glacially modified waters exported from the fjord. The noble gas analysis reveals the source waters entrained: the majority (88%) of the glacially

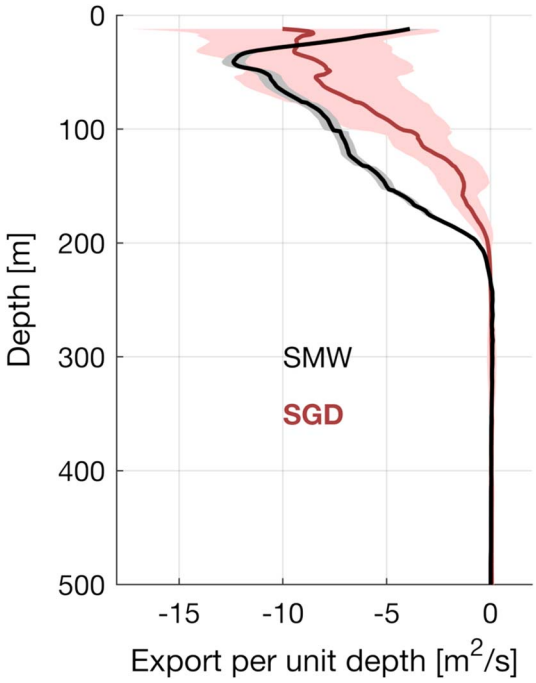

Figure 4. Vertical structure of meltwater export. Transport per unit depth of subglacial discharge and submarine meltwater across the midfjord section in Sermilik. Shading indicates uncertainty following from the error in the water mass analysis. The export maximum is at 40 m, and 50% of the transport occurs below 65 m. SMW = submarine meltwater; SGD = subglacial discharge.

modified water is formed from Atlantic Water upwelled from the deep fjord (Figure 3l). Thus, it is the deepest water mass in the fjord that contributes most substantially to the properties of the glacially modified water that is produced and exported from Sermilik (total export of 74,000 $m^3\ s^{-1}$).

In classical estuarine circulation, turbulence from tides and winds mixes surface buoyancy downward, setting up a pressure gradient that drives an exchange flow with dense inflow at depth and buoyant outflow at the surface (Geyer & MacCready, 2014). An analogous circulation arises from glacial buoyancy forcing; however, the buoyancy forcing is applied at depth along the ice-ocean boundary, with convective instability playing the role of tides and wind in driving mixing (Straneo & Cenedese, 2015). The distribution of Atlantic Water in the fjord, with high concentrations reaching to the surface, is quantitative evidence of a deep overturning cell comprised of the estuarine exchanged flow closed by the mixing in convective plumes along the ice-ocean boundaries.

The difference between classical and glacial estuarine circulation is important to proper representation of glacial freshwater in models: if meltwater is modeled as a surface freshwater source that is subsequently mixed down (classical estuarine circulation), the substantial upwelling of deep waters that is a dominant feature of glacial fjords like Sermilik will not occur, and the properties of the glacially modified water exported to the ocean will be too cold and fresh.

5. Summary

The input of $1,300 \pm 100\ m^3\ s^{-1}$ and $800 \pm 500\ m^3\ s^{-1}$ of submarine meltwater and subglacial discharge drives an export of 74,000 $m^3\ s^{-1}$ of glacially modified water, 88% of which is Atlantic Water upwelled from depth. The volume transport of glacially modified waters is 30 times the initial freshwater flux, highlighting the importance of entrainment and overturning in glacially modified water production. In contrast to a surface source of freshwater, submarine meltwater and subglacial discharge exit Sermilik fjord spread over 250 m (Figure 4) with a transport-weighted mean salinity of 33.24 and a temperature of 1.06 °C. The maximum transport of submarine meltwater and subglacial discharge occurs at 40 m, and half the meltwater transport occurs below 65 m (Figure 4).

Glacially modified water production in Sermilik is large enough to have significant regional impacts. The export of glacially modified waters from Sermilik amounts to 12% of the transport of similar-density shelf waters carried in the East Greenland Coastal Current (630 mSv for waters with salinity less than 34.5, Harden et al., 2014. Thus, given the substantial upwelled Atlantic Water, the glacier-driven overturning in this single fjord produces a significant redistribution of heat, salt, and other constituents (e.g., nutrients) on the Greenland shelf. Most glaciers in southeast Greenland are marine-terminating (Moon et al., 2012); therefore, the cumulative glacially modified water production via overturning of the many glacial fjords along the coast has significant potential to impact sea ice melt, ecosystems, and the properties of the East Greenland Coastal Current.

The noble gas measurements presented here offer a comprehensive picture of the spreading and transformation of submarine meltwater and subglacial discharge. Concentration fields make synoptic measurements of the export of glacial meltwater types possible, highlighting the glacial-driven overturning and upwelling. The noble gas tracers allow us to identify the primary water mass that is incorporated into the glacially modified waters as Atlantic Water. The results highlight the difference between the observed properties of Greenland's meltwater relative to their current representation in large-scale numerical models. As with previous tracer studies in small (Beaird et al., 2015) and large (Beaird et al., 2017) West Greenland glacial fjords, these observations highlight the dominant role of entrainment and upwelling in setting the properties of the glacially modified waters emanating from Greenland. Unlike the West Greenland sites where shallow sills block deep Atlantic Waters from the ice edge and intermediate waters are entrained into the glacially modified water (Beaird et al., 2015, 2017), Sermilik fjord has no shallow sill and the deepest Atlantic Waters are the main constituent entrained into the glacially modified water.

Much of Greenland's ice mass loss is routed to marine-terminating glaciers. Therefore, it is likely that the majority of Greenland's anomalous meltwater, both subglacial discharge and submarine melt, enters the regional ocean having been significantly modified by upwelling—with a larger volume transport and increased salinity (decreased buoyancy anomaly) as illuminated by the noble gas measurements reported here. Greenland freshwater forcing therefore needs better representation in numerical models to understand/predict its influence on the Atlantic Meridional Overturning Circulation.

Acknowledgments
We would like to thank Kevin Cahill and Dempsey Lott of the Isotope Geochemistry Facility at WHOI for the noble gas sample analysis. We also thank Brice Loose and an anonymous reviewer who helped improve the manuscript. This work was supported by a grant from the National Science Foundation (NSF OCE-1536856). Ship-based CTD data are freely available from the NOAA National Centers for Environmental Information at the Web address: http://accession.nodc.noaa.gov/0171277. Noble gas data are freely available at the Biological and Chemical Oceanography Data Management Office (BCO-DMO, https://www.bco-dmo.org/project/732806).

References

Bamber, J., van den Broeke, M. R., Ettema, J., Lenaerts, J., & Rignot, E. (2012). Recent large increases in freshwater fluxes from Greenland into the North Atlantic. *Geophysical Research Letters*, *39*, L19501. https://doi.org/10.1029/2012GL052552

Beaird, N., Straneo, F., & Jenkins, W. J. (2015). Spreading of Greenland meltwaters in the ocean revealed by noble gases. *Geophysical Research Letters*, *42*, 7705–7713. https://doi.org/10.1002/2015GL065003

Beaird, N. L., Straneo, F., & Jenkins, W. (2017). Characteristics of meltwater export from Jakobshavn Isbræand Ilulissat Icefjord. *Annals of Glaciology*, *74*, 107–117. https://doi.org/10.1017/aog.2017.19

Carroll, D., Sutherland, D. A., Shroyer, E. L., Nash, J. D., Catania, G. A., & Stearns, L. A. (2015). Modeling turbulent subglacial meltwater plumes: Implications for fjord-scale buoyancy-driven circulation. *Journal of Physical Oceanography*, *45*(8), 2169–2185. https://doi.org/10.1175/JPO-D-15-0033.1

Chu, V. W. (2014). Greenland ice sheet hydrology: A review. *Progress in Physical Geography*, *38*(1), 19–54. https://doi.org/10.1177/0309133313507075

Enderlin, E. M., Hamilton, G. S., Straneo, F., & Sutherland, D. A. (2016). Iceberg meltwater fluxes dominate the freshwater budget in Greenland's iceberg-congested glacial fjords. *Geophysical Research Letters*, *43*, 11,287–11,294. https://doi.org/10.1002/2016GL070718

Enderlin, E. M., Howat, I. M., & Jeong, S. (2014). An improved mass budget for the Greenland ice sheet. *Geophysical Research Letters*, *41*, 866–872. https://doi.org/10.1002/2013GL059010

Fettweis, X., Franco, B., Tedesco, M., van Angelen, J. H., Lenaerts, J. T. M., van den Broeke, M. R., & Gallée, H. (2012). Estimating Greenland ice sheet surface mass balance contribution to future sea level rise using the regional atmospheric climate model MAR. *The Cryosphere Discussions*, *6*, 3101–3147.

Fichefet, T. (2003). Implications of changes in freshwater flux from the Greenland ice sheet for the climate of the 21st century. *Geophysical Research Letters*, *30*(17), 1911. https://doi.org/10.1029/2003GL017826

Geyer, W. R., & MacCready, P. (2014). The estuarine circulation. *Annual Review of Fluid Mechanics*, *46*(1), 175–197. https://doi.org/10.1146/annurev-fluid-010313-141302

Harden, B. E., Straneo, F., & Sutherland, D. A. (2014). Moored observations of synoptic and seasonal variability in the East Greenland Coastal Current. *Journal of Geophysical Research: Oceans*, *119*, 8838–8857. https://doi.org/10.1002/2014JC010134

Hohmann, R., Schlosser, P., Jacobs, S., Ludin, A., & Weppernig, R. (2002). Excess helium and neon in the southeast Pacific: Tracers for glacial meltwater. *Journal of Geophysical Research*, *107*(C11), 3198. https://doi.org/10.1029/2000JC000378

Hu, A., Meehl, G. A., Han, W., & Yin, J. (2011). Effect of the potential melting of the Greenland Ice Sheet on the Meridional Overturning Circulation and global climate in the future. *Deep Sea Research Part II: Topical Studies in Oceanography*, *58*(17-18), 1914–1926. https://doi.org/10.1016/j.dsr2.2010.10.069

Jackson, R. H., & Straneo, F. (2016). Heat, salt, and freshwater budgets for a glacial fjord in Greenland. *Journal of Physical Oceanography*, *46*(9), 2735–2768. https://doi.org/10.1175/JPO-D-15-0134.1

Jackson, R. H., Shroyer, E. L., Nash, J. D., Sutherland, D. A., Carroll, D., Fried, M. J., et al. (2017). Near-glacier surveying of a subglacial discharge plume: Implications for plume parameterizations. *Geophysical Research Letters*, *44*, 6886–6894. https://doi.org/10.1002/2017GL073602

Jackson, R. H., Straneo, F., & Sutherland, D. A. (2014). Externally forced fluctuations in ocean temperature at Greenland glaciers in non-summer months. *Nature Geoscience*, *7*(7), 503–508. https://doi.org/10.1038/ngeo2186

Jungclaus, J. H., Haak, H., Esch, M., Roeckner, E., & Marotzke, J. (2006). Will Greenland melting halt the thermohaline circulation? *Geophysical Research Letters*, *33*, L17708. https://doi.org/10.1029/2006GL026815

Lazier, J. R. (1980). Oceanographic conditions at Ocean Weather Ship Bravo, 1964–1974. *Atmosphere-Ocean*, *18*(3), 227–238. https://doi.org/10.1080/07055900.1980.9649089

Loose, B., & Jenkins, W. J. (2014). The five stable noble gases are sensitive unambiguous tracers of glacial meltwater. *Geophysical Research Letters*, *41*, 2835–2841. https://doi.org/10.1002/2013gl058804

Lozier, M. S. (2012). Overturning in the North Atlantic. *Annual Review of Marine Science*, *4*(1), 291–315. https://doi.org/10.1146/annurev-marine-120710-100740

Manabe, S. (1995). Simulation of abrupt climate change induced by freshwater input to the North Atlantic Ocean. *Nature*, *378*, 165–167.

Mankoff, K. D., Straneo, F., Cenedese, C., Das, S. B., Richards, C. G., & Singh, H. (2016). Structure and dynamics of a subglacial discharge plume in a Greenlandic fjord. *Journal of Geophysical Research: Oceans*, *121*, 8670–8688. https://doi.org/10.1002/2016JC011764

Mernild, S. H., Howat, I. M., Ahn, Y., Liston, G. E., Steffen, K., Jakobsen, B. H., et al. (2010). Freshwater flux to Sermilik Fjord, SE Greenland. *The Cryosphere*, *4*(4), 453–465. https://doi.org/10.5194/tc-4-453-2010

Moon, T., Joughin, I., Smith, B., & Howat, I. (2012). 21st-century evolution of Greenland outlet glacier velocities. *Science*, *336*(6081), 576–578. https://doi.org/10.1126/science.1219985

Moon, T., Sutherland, D. A., Carroll, D., Felikson, D., Kehrl, L., & Straneo, F. (2018). Subsurface iceberg melt key to Greenland fjord freshwater budget. *Nature Geoscience*, *11*, 49–54. https://doi.org/10.1038/s41561-017-0018-z

Noël, B. P. Y., van de Berg, W. J., Machguth, H., Lhermitte, S., Howat, I., Fettweis, X., & van den Broeke, M. R. (2016). A daily, 1 km resolution data set of downscaled Greenland ice sheet surface mass balance. *The Cryosphere*, *10*(5), 2361–2377. https://doi.org/10.5194/tc-10-2361-2016

Schlosser, P. (1986). Helium: A new tracer in Antarctic oceanography. *Nature*, *321*, 233–235.

Sciascia, R., Straneo, F., Cenedese, C., & Heimbach, P. (2013). Seasonal variability of submarine melt rate and circulation in an East Greenland fjord. *Journal of Geophysical Research: Oceans*, *118*, 2492–2506. https://doi.org/10.1002/jgrc.20142

Shepherd, A., Ivins, E. R., Barletta, G. A, Bentley, M. J., Bettadpur, S., Briggs, K. H., et al. (2012). A reconciled estimate of ice-sheet mass balance. *Science*, *338*(6111), 1183–1189. https://doi.org/10.1126/science.1228102

Straneo, F., & Cenedese, C. (2015). The dynamics of Greenland's glacial fjords and their role in climate. *Annual Review of Marine Science*, *7*(1), 89–112. https://doi.org/10.1146/annurev-marine-010213-135133

Straneo, F., Curry, R. G., Sutherland, D. A., Hamilton, G. S., Cenedese, C., Våge, K., & Stearns, L. A. (2011). Impact of fjord dynamics and glacial runoff on the circulation near Helheim Glacier. *Nature Geoscience*, *4*(5), 322–327. https://doi.org/10.1038/ngeo1109

Straneo, F., Hamilton, G. S., Sutherland, D. A., Stearns, L. A., Davidson, F., Hammill, M. O., et al. (2010). Rapid circulation of warm subtropical waters in a major glacial fjord in East Greenland. *Nature Geoscience*, *3*(3), 182–186. https://doi.org/10.1038/ngeo764

Straneo, F., Sutherland, D. A., Holland, D., Gladish, C., Hamilton, G. S., Johnson, H., et al. (2012). Characteristics of ocean waters reaching Greenland's glaciers. *Annals of Glaciology*, *53*(60), 202–210. https://doi.org/10.3189/2012AoG60A059

Sutherland, D. A., & Pickart, R. S. (2008). The East Greenland Coastal Current: Structure, variability, and forcing. *Progress in Oceanography*, *78*(1), 58–77. https://doi.org/10.1016/j.pocean.2007.09.006

Sutherland, D. A., Pickart, R. S., Peter Jones, E., Azetsu-Scott, K., Jane Eert, A., & Ólafsson, J. (2009). Freshwater composition of the waters off southeast Greenland and their link to the Arctic Ocean. *Journal of Geophysical Research*, *114*, C05020. https://doi.org/10.1029/2008JC004808

Sutherland, D. A., & Straneo, F. (2012). Estimating ocean heat transports and submarine melt rates in Sermilik Fjord, Greenland, using lowered acoustic Doppler current profiler (LADCP) velocity profiles. *Annals of Glaciology*, *53*(60), 50–58. https://doi.org/10.3189/2012AoG60A050

Tomczak, M., & Large, D. G. B. (1989). Optimum multiparameter analysis of mixing in the thermocline of the eastern Indian Ocean. *Journal of Geophysical Research*, *94*(C11), 16,141–16,149. https://doi.org/10.1029/JC094iC11p16141

van den Broeke, M. R., Bamber, J., Ettema, J., Rignot, E., Schrama, E., van, W. J., et al. (2009). Partitioning recent Greenland mass loss. *Science*, *326*(5955), 984–986. https://doi.org/10.1126/science.1178176

Weijer, W., Maltrud, M. E., Hecht, M. W., Dijkstra, H. A., & Kliphuis, M. A. (2012). Response of the Atlantic Ocean circulation to Greenland Ice Sheet melting in a strongly-eddying ocean model. *Geophysical Research Letters*, *39*, L09606. https://doi.org/10.1029/2012GL051611